64782-RG-2

SUPPLEMENTARY INFORMATION

Loss of SPARC in bladder cancer enhances carcinogenesis and progression

Neveen Said [1#], Henry F Frierson [2], Marta Sanchez-Carbayo [3], Rolf A. Brekken[4] and Dan Theodorescu [1,5,6*]

[1] Departments of Urology and [2] Pathology, University of Virginia,

[3] Spanish National Cancer Institute (CNIO),

[4] Departments of Surgery and Pharmacology, University of Texas Southwestern Medical Center,

[5] Departments of Surgery and Pharmacology University of Colorado, and

[6] University of Colorado Comprehensive Cancer Center.

[#] Current address: Department of radiation Oncology, University of Virginia.

SUPPLEMENTARY FIGURE LEGENDS

Supplement Figure 1. Loss of SPARC enhances BBN-induced cell cycle dysregulation in murine urothelium. Quantification of Western blot analysis of 25μg protein of murine urothelium dissected from $SP^{+/+}$ and $SP^{-/-}$ bladders with the indicated pathology for cell cycle proteins cyclins A, D1 and E, and their inhibitors p21 and p27 shown in **Figure 5B.** Protein loading was verified by probing the membranes with tubulin. Bars represent the fold change of the relative band densities normalized to the corresponding tubulin with the normalized value of the normal urothelium set at 1 for each genotype. *P<0.05, two-tail Student t-test.

Supplement Figure 2. Characterization of primary urothelial and stromal cell populations. A-B. Protein lysates (20ug) of primary normal urothelium (NU) and urothelial cancer (UC); and normal fibroblasts (NF) and cancer associated fibroblasts (CAF), from $SP^{-/-}$ and $SP^{+/+}$ were loaded on SDS-PAGE and transferred to PVDF membranes. NU and UC were characterized by antibodies against SPARC, epithelial marker, pan-keratin, or fibroblastic markers, vimentin and α-smooth muscle actin (α-sma).

Supplement Figure 3. Bladder carcinogenesis in $SP^{-/-}$ mice is associated with increased activation of NFκB and p38-JNK-AP-1. A. Quantification of Western blot analysis of bladder tissues dissected from $SP^{+/+}$ and $SP^{-/-}$ mice with the indicated pathology for phosphor and total NFκB, p38, SAPK/JNK, cJun as shown in **Figure 6A.** Bars represent the means ± SEM of the relative band densities of the phosphorylated/total protein and normalized to the corresponding tubulin. *P<0.05, two-tail Student t-test. **B.** Scoring of immunostaining of phspho-p65 NFκB and phosphor-cJun as shown in **Figure 6B,** were performed on two arbitrary scores for intensity and frequency of immunostaining of each protein in the cytoplasm and nuclei of urothelium and stromal compartments in the indicated groups. Scores were transformed into composite expression scores (CES) as described in the Materials and Methods. Bars represent the mean ± SEM of scores for each group (n=15). *Correlation of composite scores in association with tumor grades by Kruskal-Wallis' one way ANOVA followed by Dunn's multiple comparison post-hoc test. **Correlation of composite scores between indicated groups by one-way ANOVA with Bonferroni multiple comparison post-hoc test.

Supplement Figure 4. Enhanced inflammation in $SP^{+/+}$ and $SP^{-/-}$bladders. A. Levels of cytokines were determined in bladder lysates by ELISA as per manufacturer's instructions. Bars

are means ± SEM (n=4). *P<0.05 between $SP^{-/-}$ and $SP^{+/+}$, two-tail Student's t-test. **P<0.05 between different cohorts, one way Analysis of Variance (ANOVA). **B.** Macrophage marker mac-1 (magnification 200x). Bars represent means ± SEM of mac1 positive cells counted in 6 random HPF/slide (n=5 animals of each genotype/group); magnification, 100x.*P<0.05 comparing $SP^{-/-}$ and $SP^{+/+}$, two-tail Student's t-test. **P<0.05, one way ANOVA.

Supplement Figure 5. Characterization of primary on $SP^{+/+}$ and $SP^{-/-}$ macrophages. A. Proliferation of $SP^{+/+}$ and $SP^{-/-}$ macrophages (left) was determined by CyQuant assay 72h after plating in CGM (n=4). The effect of exogenous murine SPARC (0-40μg/ml) and over-expression of SPARC (middle) on $SP^{+/+}$ macrophages proliferation. Bars represent means ± SEM of a representative of 3 independent experiments performed in quadruplicates. **B.** The expression of SPARC protein in differentiating $SP^{+/+}$ macrophages (as described in material and methods) at the indicated time points. Equal protein loading was confirmed by re-probing blots with tubulin. **C-D.** Activation of AP-1 and NFκB promoters in primary $SP^{+/+}$ and $SP^{-/-}$ macrophages (Macs), under basal growth conditions in single cultures, was determined by luciferase reporter assays as described above. **E.** Cytokine production was measured in CM of primary $SP^{-/-}$ and $SP^{+/+}$ Macs, in the presence or absence of 0.1% H2O2 for 48h. Bars represent means ± SEM (n=3) fold increase in the levels of H_2O_2-treated over non-stimulated (NS) Macs. **F.** H_2O_2 generation by $SP^{+/+}$ and $SP^{-/-}$ Macs was determined by DCF fluorescence intensity 24h after stimulation with CM of $SP^{+/+}$ and $SP^{-/-}$ UCs. Bars represent mean±SEM of three independent experiments performed in quadruplicates. *P<0.05 between $SP^{-/-}$ and $SP^{+/+}$ Macs (n=4), two-tail Student's t-test.

Supplement Figure 6. Characterization of primary $SP^{+/+}$ and $SP^{-/-}$ fibroblasts. A. Proliferation of $SP^{+/+}$ and $SP^{-/-}$ NF and CAF was determined by CyQuant assay 72h after plating in CGM. In some experiments, the effect of exogenous murine SPARC (20μg/ml) on $SP^{-/-}$ NF and CAF was evaluated. Bars represent means ± SEM of a representative of 3 independent experiments performed in quadruplicates. *P<0.05. **P<0.01. **B.** The expression of SPARC protein in differentiating $SP^{+/+}$ NF stimulated by 0.1% H_2O_2, filter-sterilized SPARC-depleted CM of 72h monolayers of MB49 cells and 10nM 8-isoprostane for 10 days with replenishing fresh H_2O_2 and CM every 2 days. at the indicated time points. Equal protein loading was confirmed by re-probing blots with tubulin. **C.** $SP^{+/+}$ and $SP^{-/-}$ NF grown to confluence in 24-well plates were stimulated with either 0.1% H_2O_2 or CM as in **B.** Levels of cytokines were determined at day 10 in cell lysates by ELISA as per manufacturer's instructions. Bars are means ± SEM (n=4).

*P<0.05 between $SP^{-/-}$ and $SP^{+/+}$ CAFs. **D.** Cytokine production was measured in CM of primary $SP^{-/-}$ and $SP^{+/+}$ NF and CAF by ELISA. Bars represent mean±SEM of fold increase in CAF/NF. *P<0.05. **E.** H_2O_2 generation by $SP^{+/+}$ and $SP^{-/-}$ CAFs was determined by DCF fluorescence intensity. Bars represent mean±SEM of three independent experiments performed in quadruplicates. *P<0.05, two-tail Student's *t*-test.

Supplement Figure 7. A. Photomicrographs of representative $SP^{+/+}$ and $SP^{-/-}$ bladders of the different cohorts showing evidence of increased vascularity. **B-C.** CD31 immunostaining of $SP^{+/+}$ and $SP^{-/-}$ bladders (100x magnification). Bars represent means ± SEM of the mean vascular density (MVD, calculating the number of CD31 positivity) and mean vascular area (MVA, measuring percentage of the area of CD31 positivity) in 6 random high power fields (HPF) per slide (n=6 mice/cohort). *P<0.05 between $SP^{-/-}$ and $SP^{+/+}$ two-tail Student's t-test. **P<0.05, one way ANOVA.

Supplement Figure 8. The metastasis suppressor effect of SPARC is associated with decreased inflammation in the lungs. A. The levels of inflammatory cytokines in lung tissue lysates corresponding to the bladders in the cohorts of **Figure 6D.** Bars are means ± SEM (n=4). *P<0.05 between $SP^{-/-}$ and $SP^{+/+}$, unpaired two-tail Student's *t*-test. **P<0.05 between different cohorts, one way ANOVA. **B.** Mac1 immunostaining in metastatic nodules in BBN-induced lung metastases in $SP^{-/-}$ and $SP^{+/+}$ lungs. Bars represent means ± SEM of the number of tumor infiltrating macrophages within and around metastases counted in 6 random HPF/section (4 animals/group; magnification 200x). *P<0.05 between $SP^{-/-}$ and $SP^{+/+}$, unpaired two-tail Student's *t*-test.

Supplement Figure 9. Host-SPARC inhibits MB49 bladder cancer cell growth and metastasis. A. Mac1 immunostaining of MB49 SC tumors dissected 14 days after injection in $SP^{-/-}$ and $SP^{+/+}$ mice. Bars represent means ± SEM of the number of TAMs in 6 random HPF/section (n=6; magnification, 100x). **B.** The mean vascular density (MVD) of SC tumors was determined by CD31 immunostaining. Bars represent means±SEM of the number of CD31-positivity counted in 6 random HPF/section (n=6; magnification,100x). *P<0.05, Student's *t*-test. **C.** H&E- stained lung sections of $SP^{-/-}$ and $SP^{+/+}$ mice harboring SC tumors of **Figure 9B.** (upper). Mac1 immunostaining of lung sections (lower); bars represent means±SEM of the number of TAMs within and around metastases counted in 6 HPF/section (n=6/group);

magnification, 200x. **D.** Inflammatory cytokines in lungs and matching SC tumors. Bars represent mean±SEM (n=3/group). *P<0.05, Student's t test, compared with $SP^{+/+}$ mice

Supplement Figure 10. Loss of tumor SPARC enhances experimental metastases: A-B. Scatter plots of incidence and multiplicity of lung metastases after tail vein injection of UMUC3, T24, T24T cells overexpressing and depleted of SPARC in nude mice. *P<0.01, χ^2 test comparing the incidence, and **P<0.01, Student's t-test, comparing the number of visible metastases. **C.** Kaplan Meier's curve showing survival of nude mice injected with UMUC3-shSP compared to UMUC3-NTsh. **D.** Photomicrographs of CMFDA-labeled UMUC3-NTsh and UMUC3-shSP cells intravenously injected in nude mice at indicated time points. Bars represent mean ± SEM of fluorescent intensity measured as described above. *P<0.05, Student's t test, compared with UMUC3-NTsh. **P<0.05, one way ANOVA.

Supplement Figure 11. A. Representative images of negative controls of SPARC immunostaining of human TMA omitting the primary antibody (magnification, 100x). **B.** Representative positive immunostaining of SPARC-positive normal human ovarian tissue presence and absence of 1 µg/ml rhSPARC (R&D Inc. # 941-SP) and, in presence and absence and 1 µg/ml human osteonectin (Haematologic Technologies Inc. # HON-0303) showing inhibition of tissue staining (magnification, 200x). **C.** SPARC IHC in $SP^{-/-}$ mouse tumor cohorts (magnification 200x). **D.** SPARC IHC of mouse tumor tissues omitting the primary antibody and in the presence of 1 µg/ml recombinant mouse SPARC (rmSPARC, R&D Inc. # 942-SP) as a competitive inhibitor (magnification 100x).

Supplement Figure 12: A simplified schematic summarizing the findings in the present study. In the multistep carcinogenesis cascade, BBN through the generation of ROS instigates differential effects on the urothelium and suburothelial stroma (macrophages and fibroblasts) and maintained by a reciprocated feed forward loop by cancer cells, macrophages and fibroblasts leading to bladder cancer progression and metastasis.

Supplement Figure 1

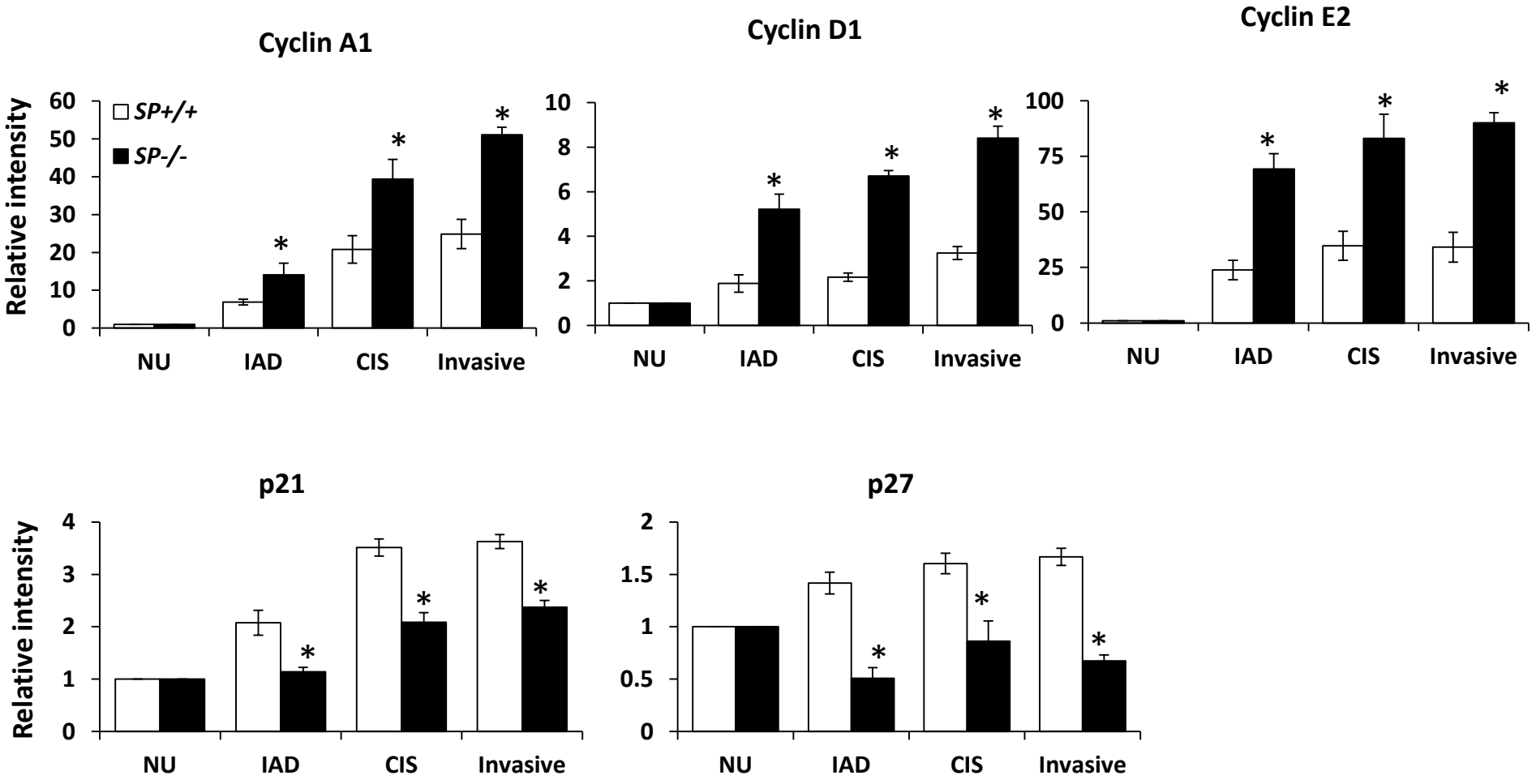

Supplement Figure 2

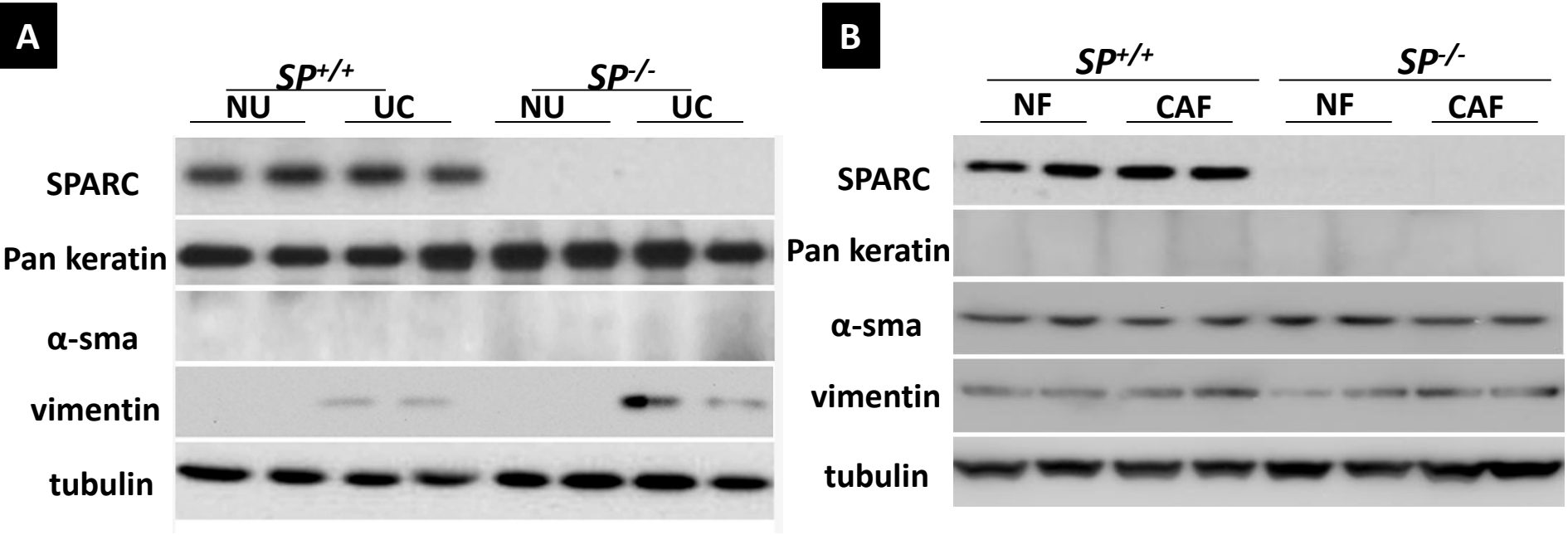

Supplement Figure 3

A

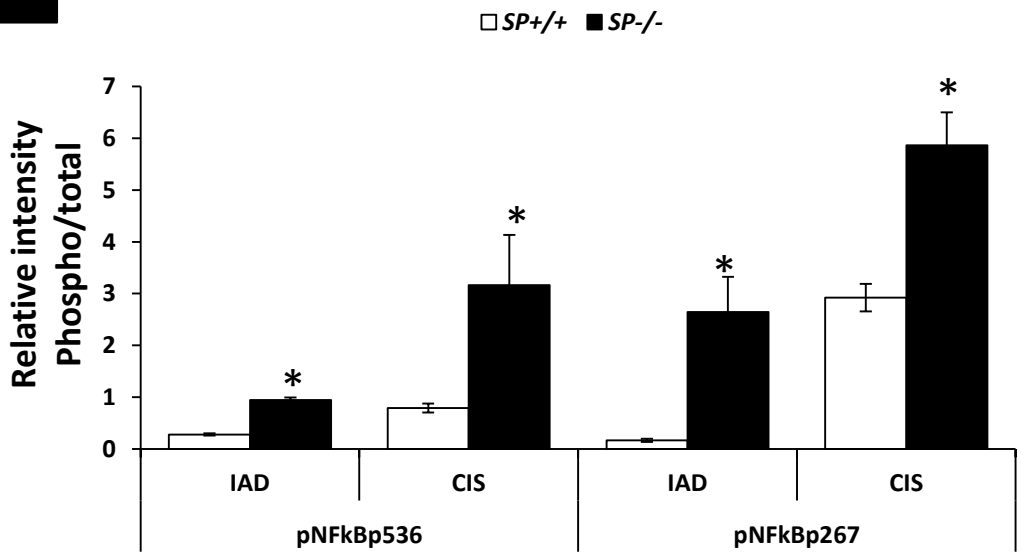

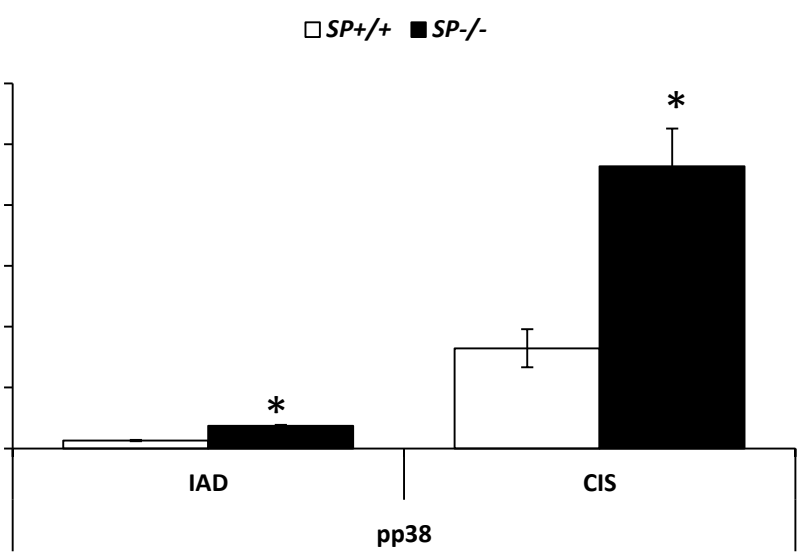

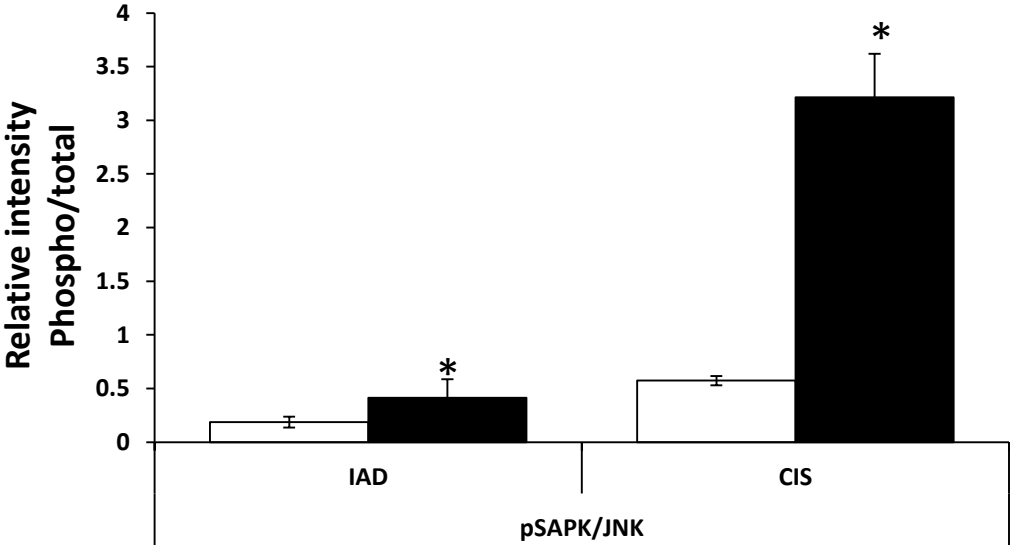

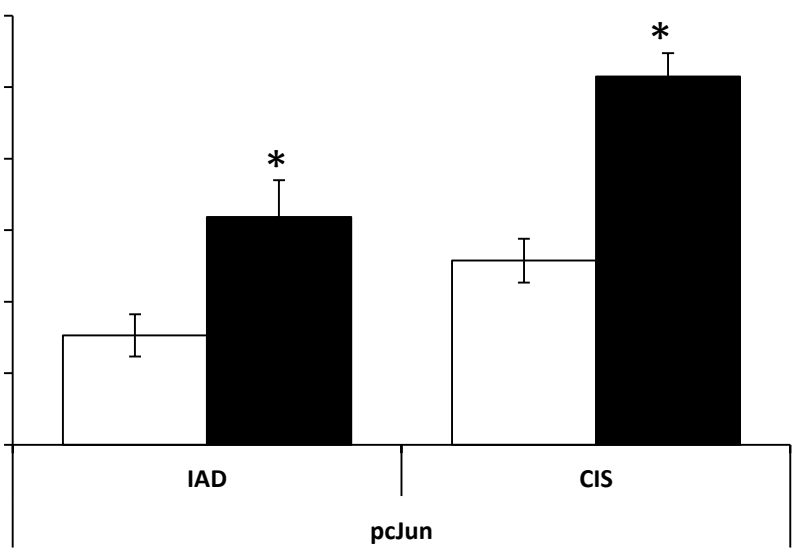

Supplement Figure 3

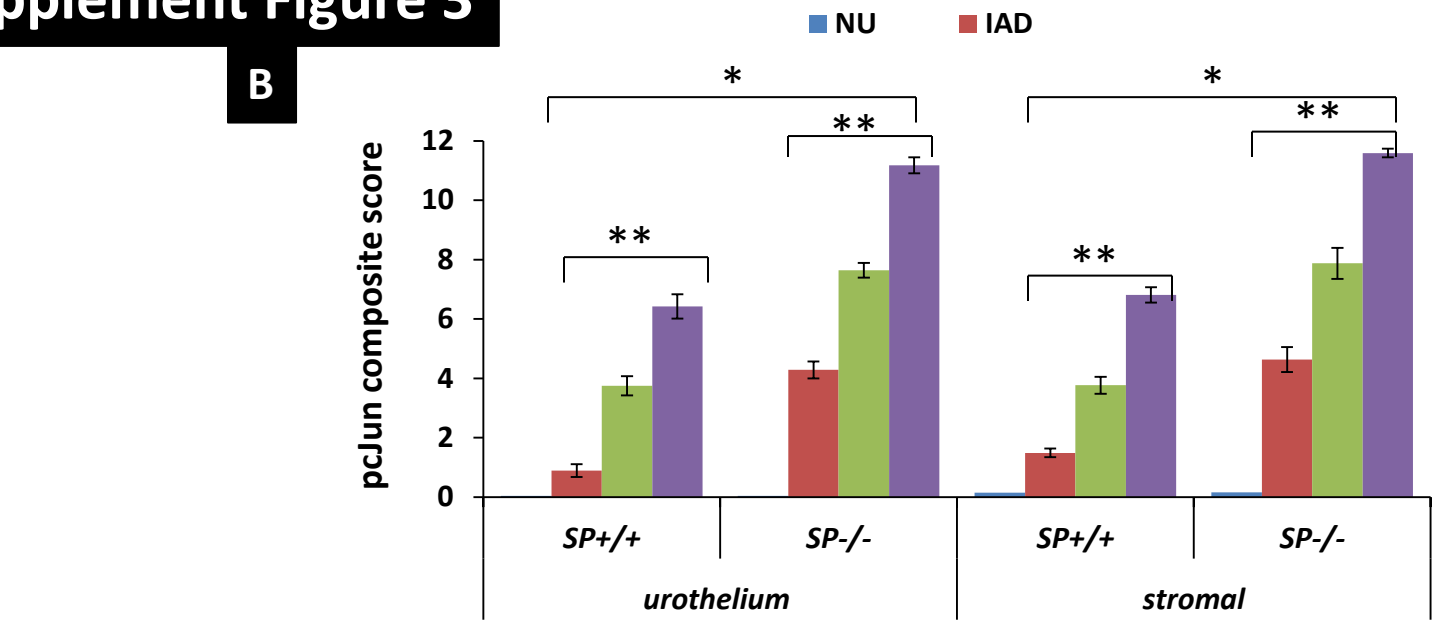

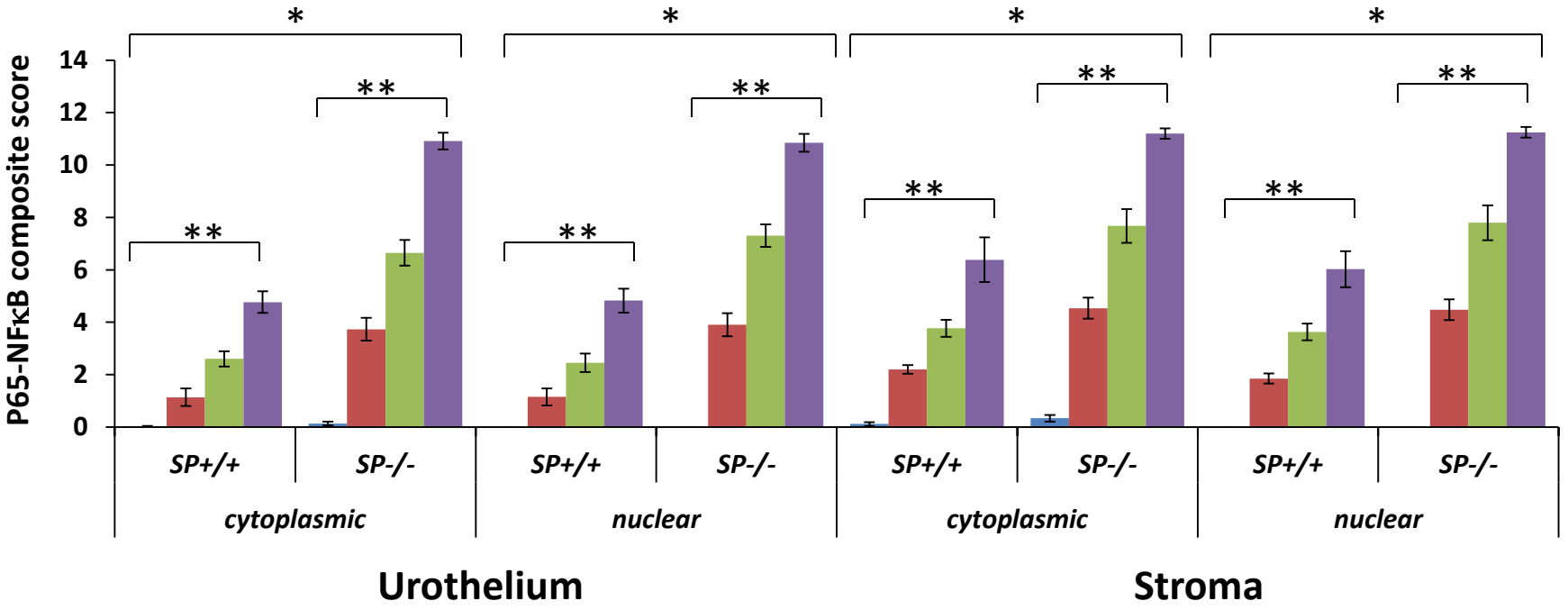

Supplement Figure 4

A

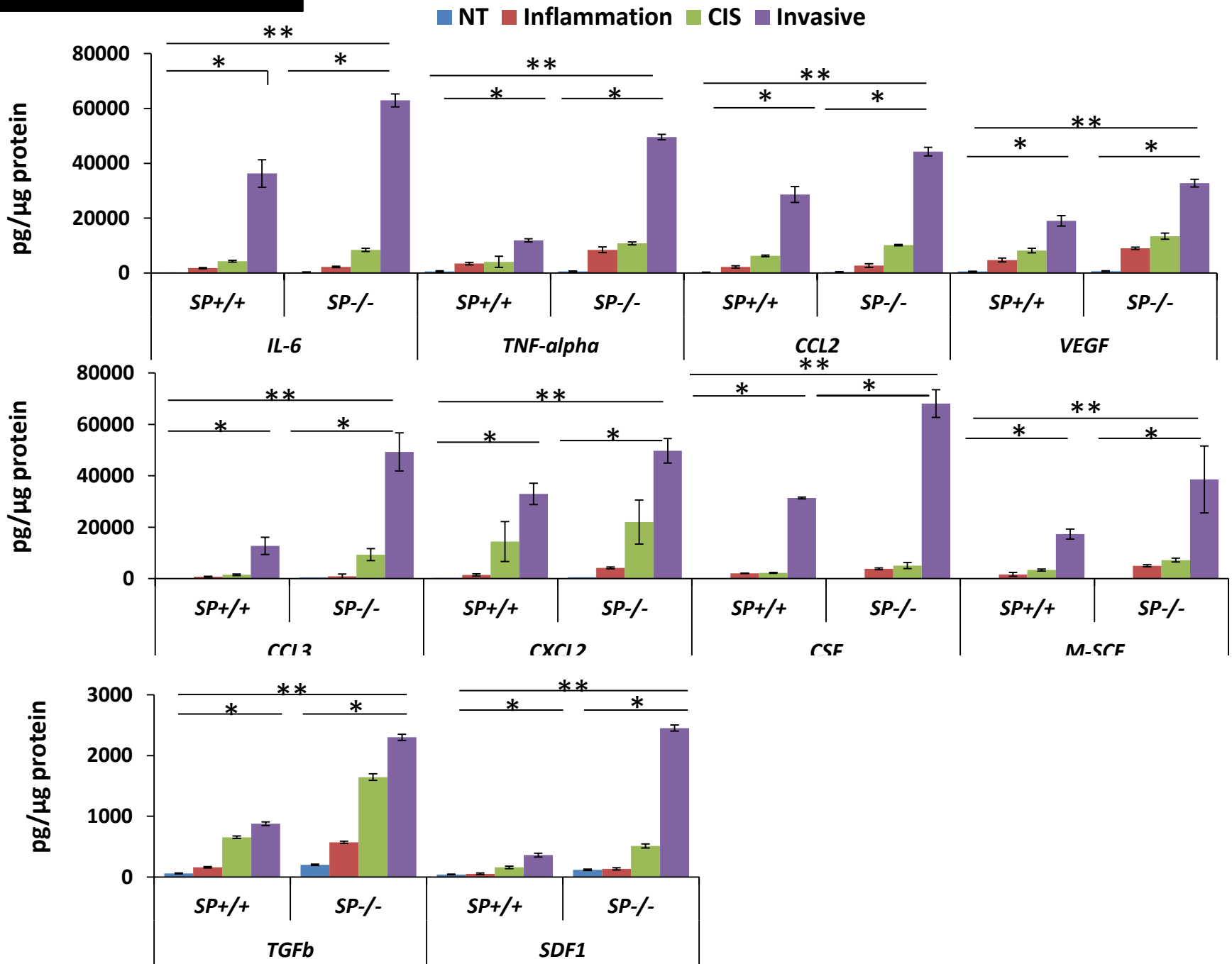

Supplement Figure 4

B

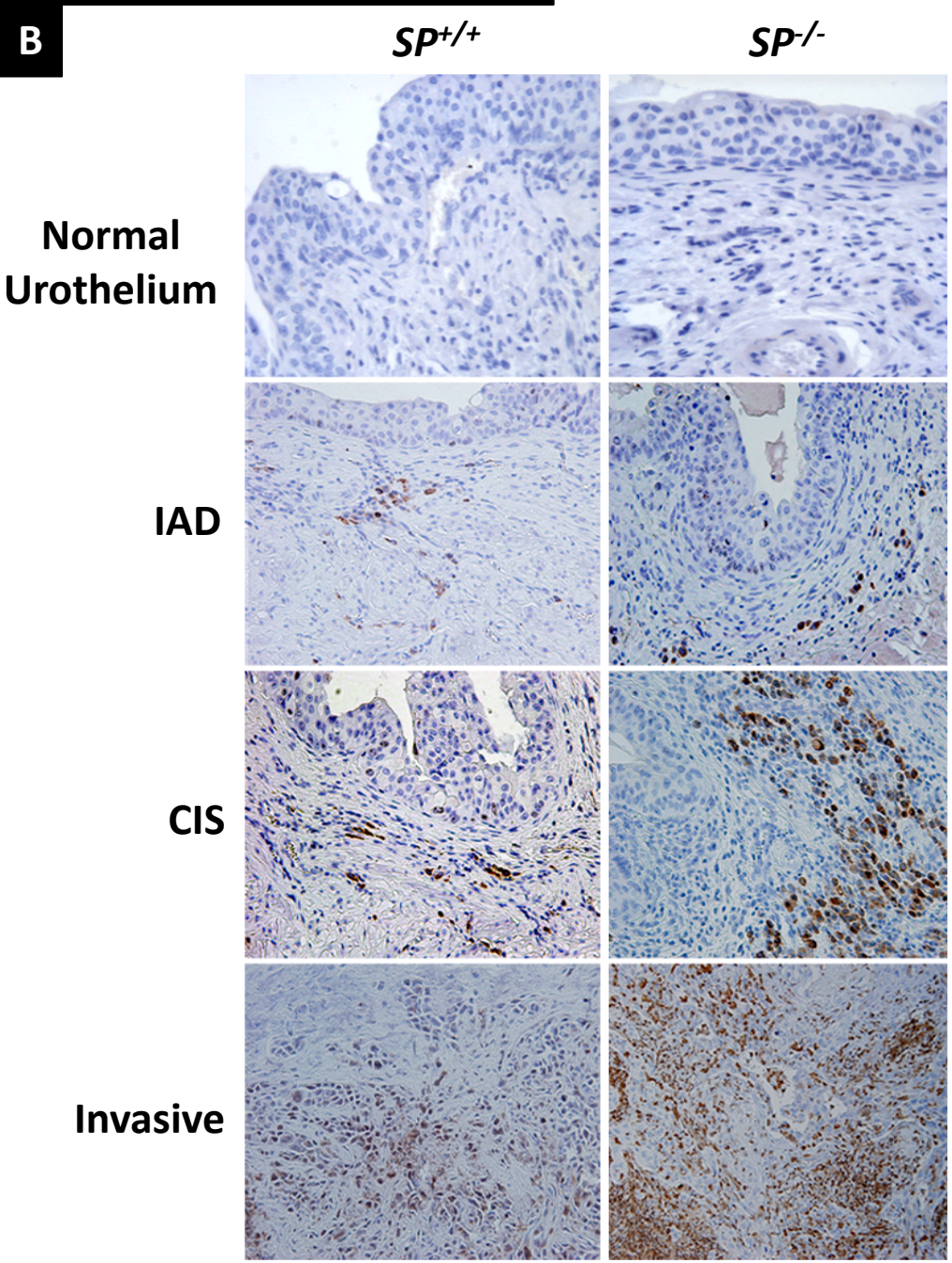

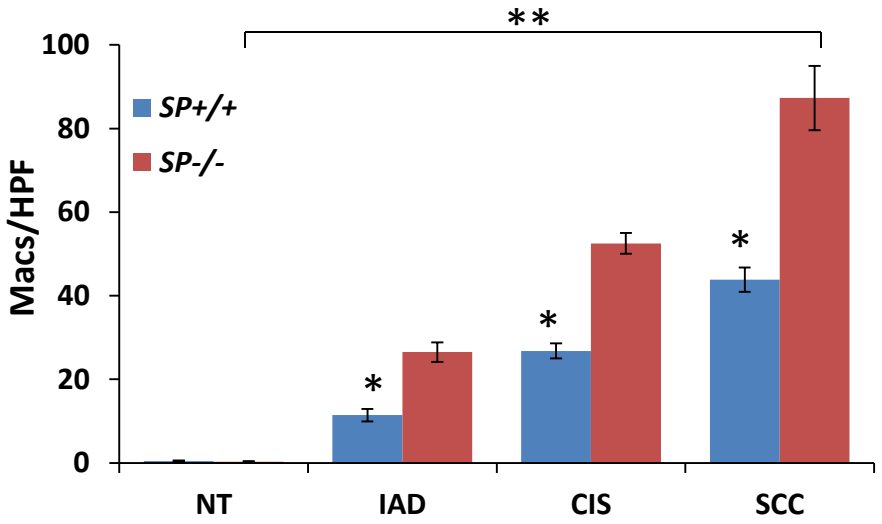

Supplement Figure 5

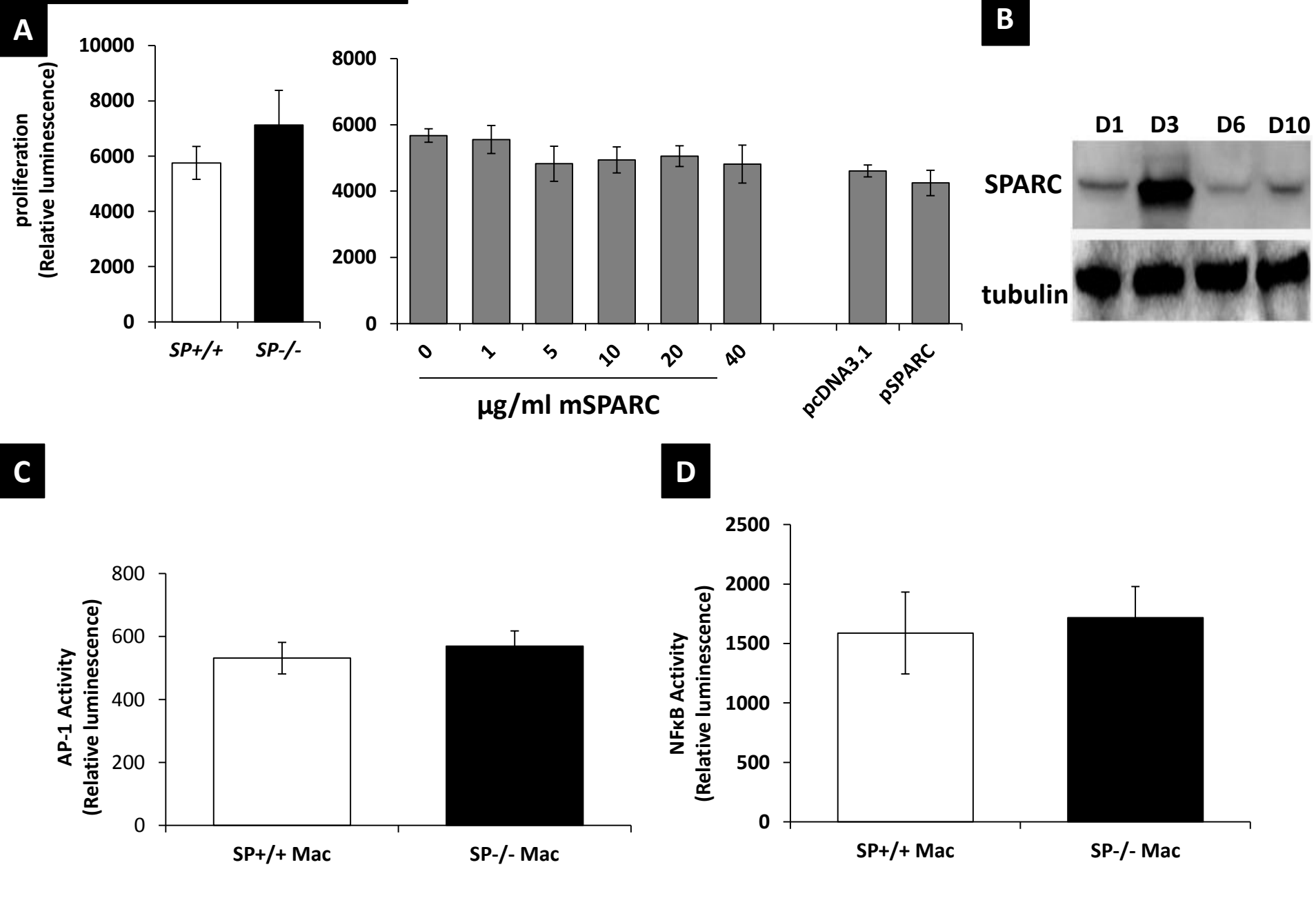

Supplement Figure 5

E

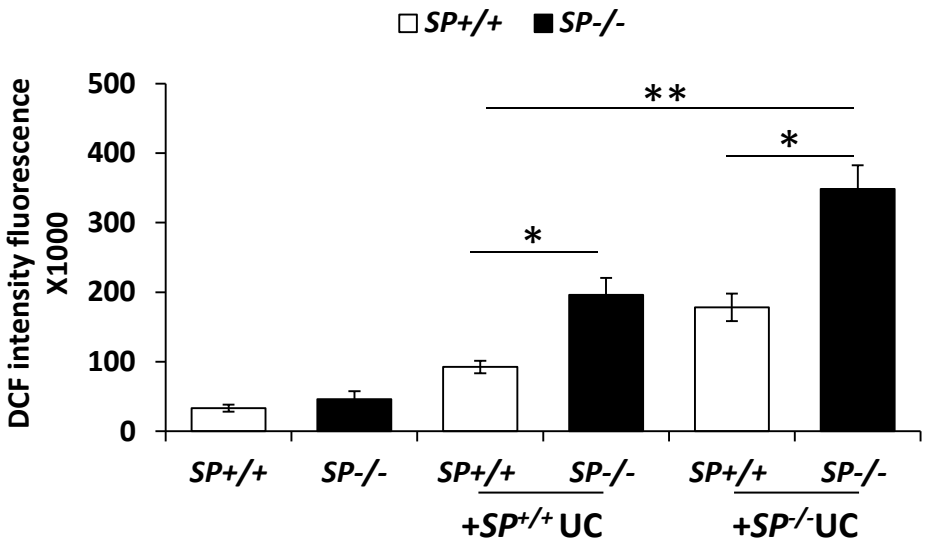

F

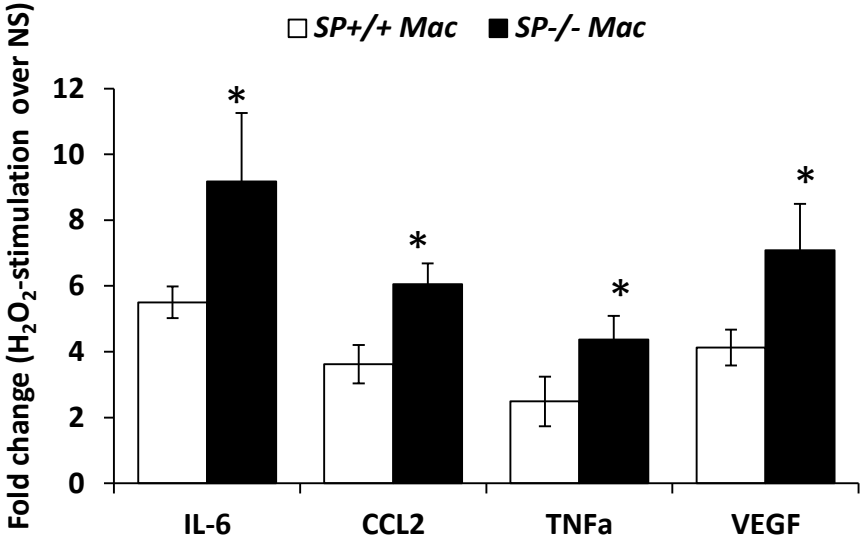

Supplement Figure 6

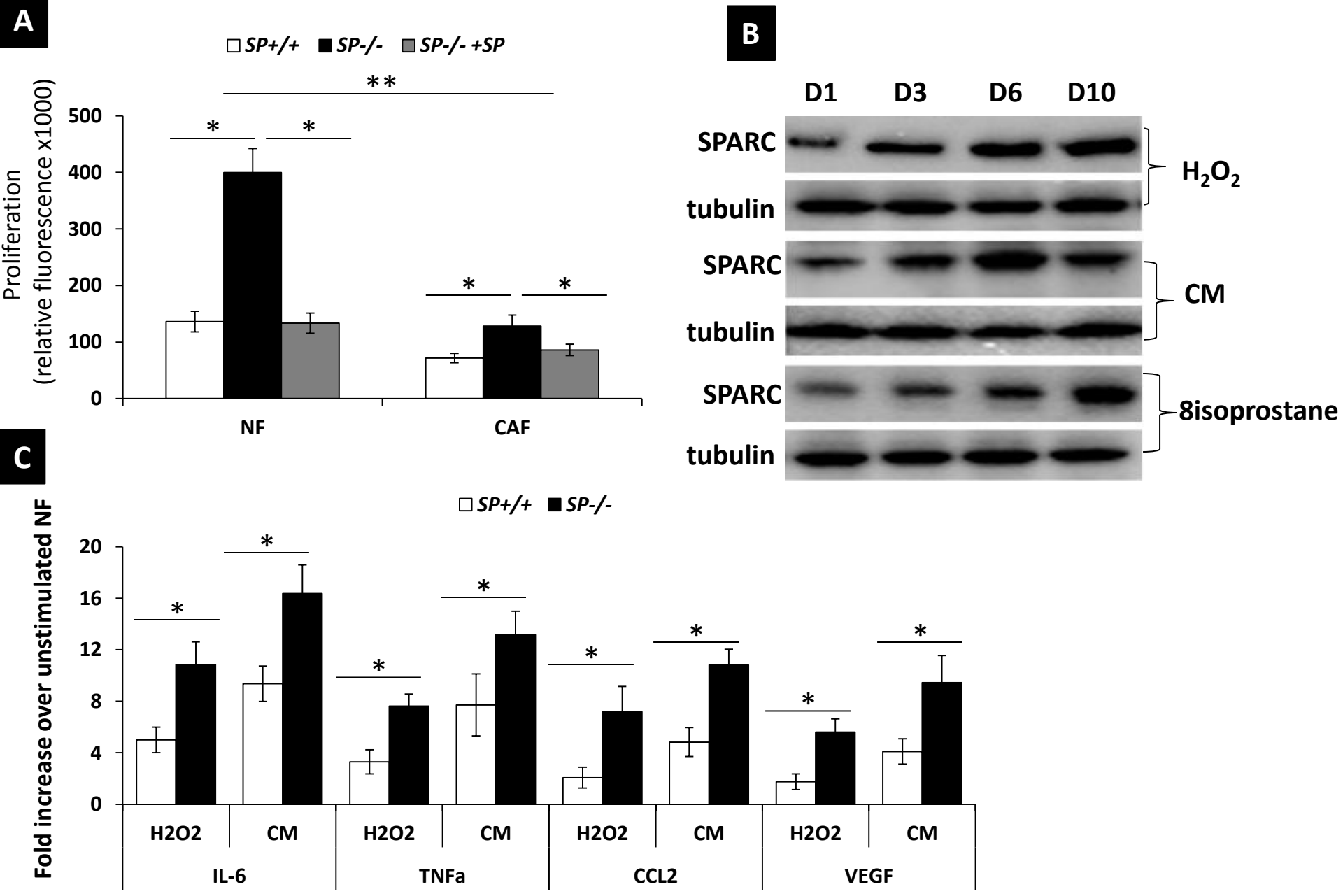

Supplement Figure 6

D

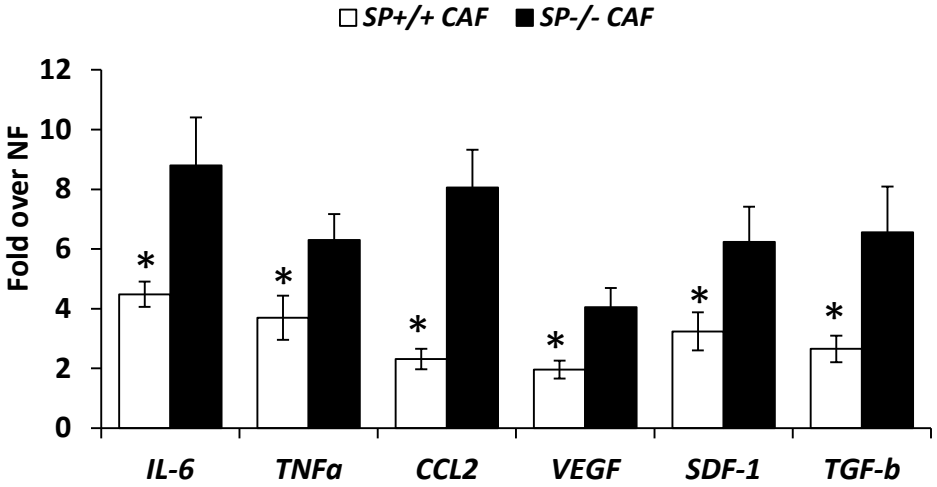

E

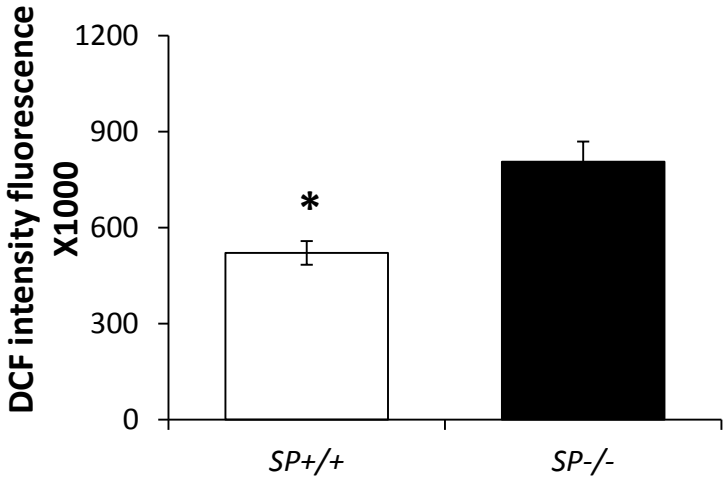

Supplement Figure 7

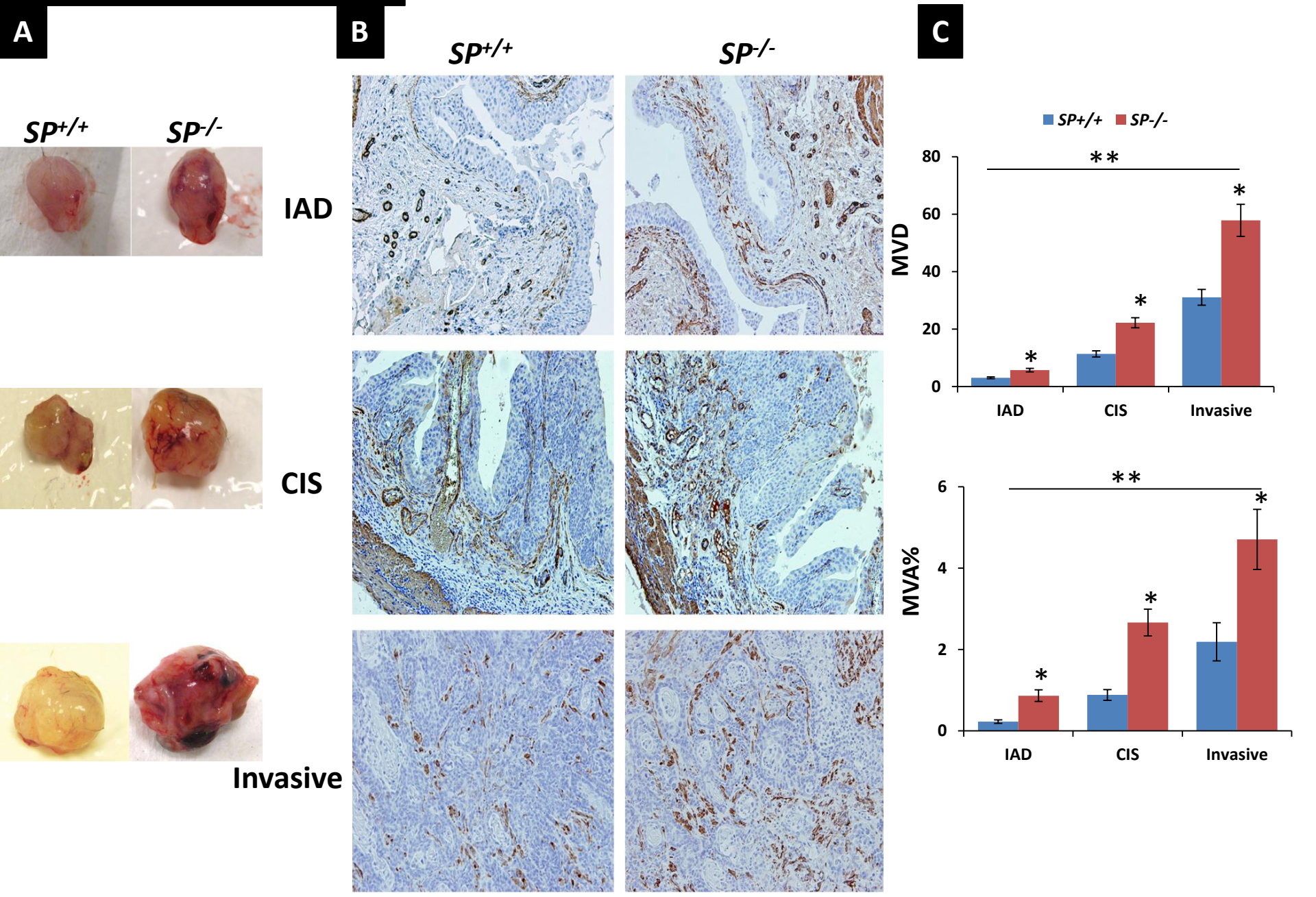

Supplement Figure 8

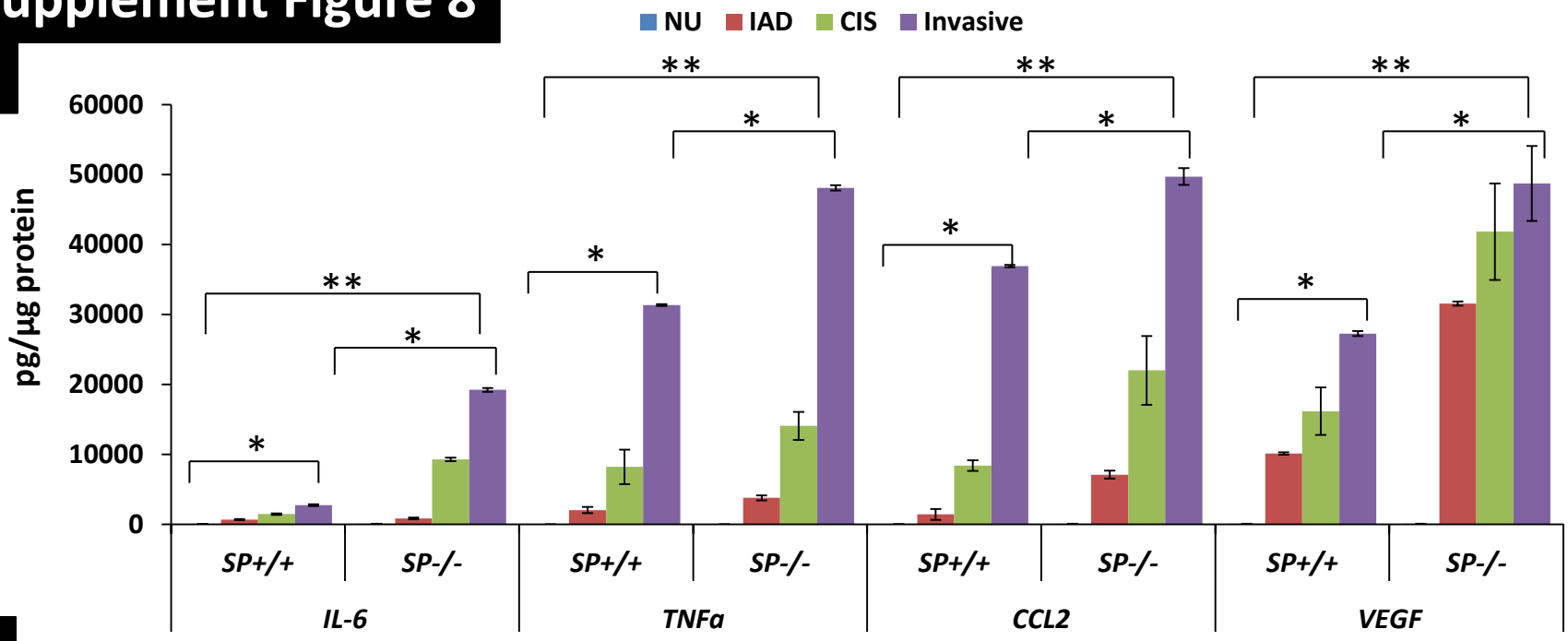

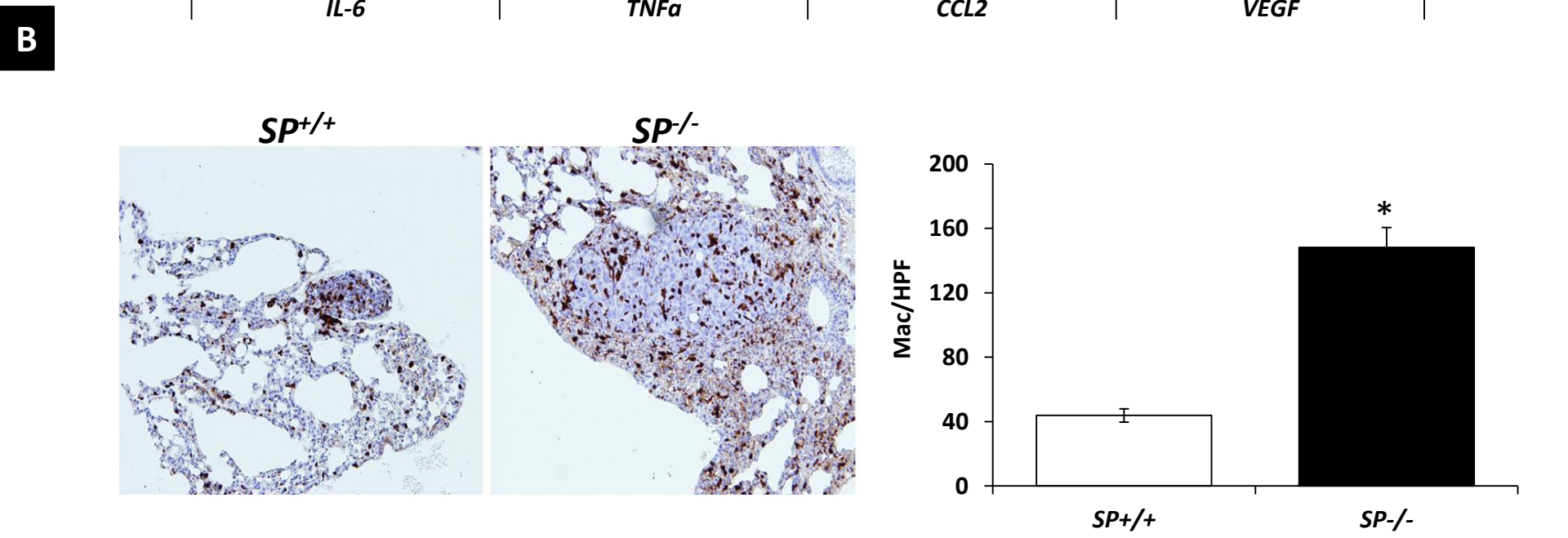

Supplement Figure 9

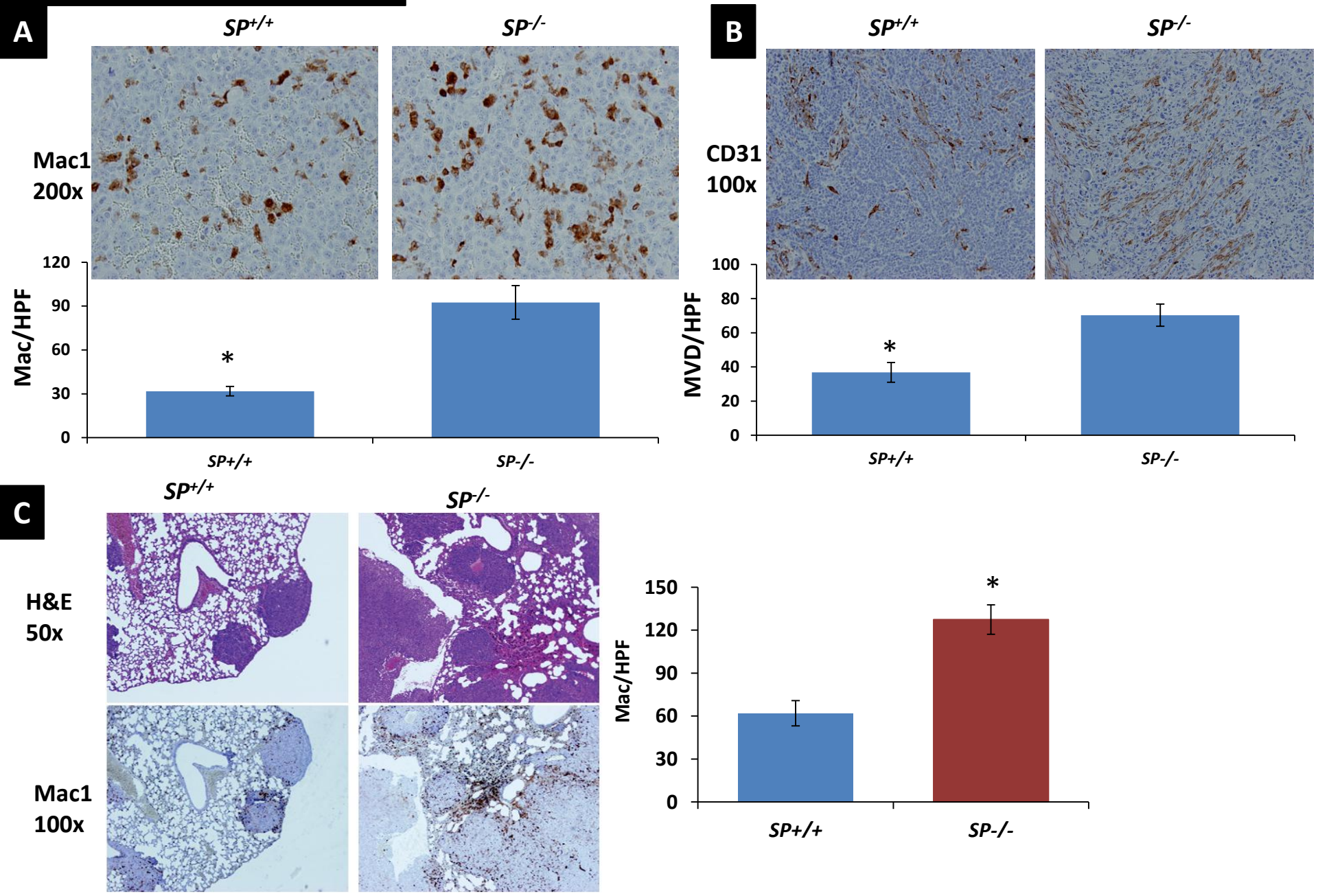

Supplement Figure 9

D

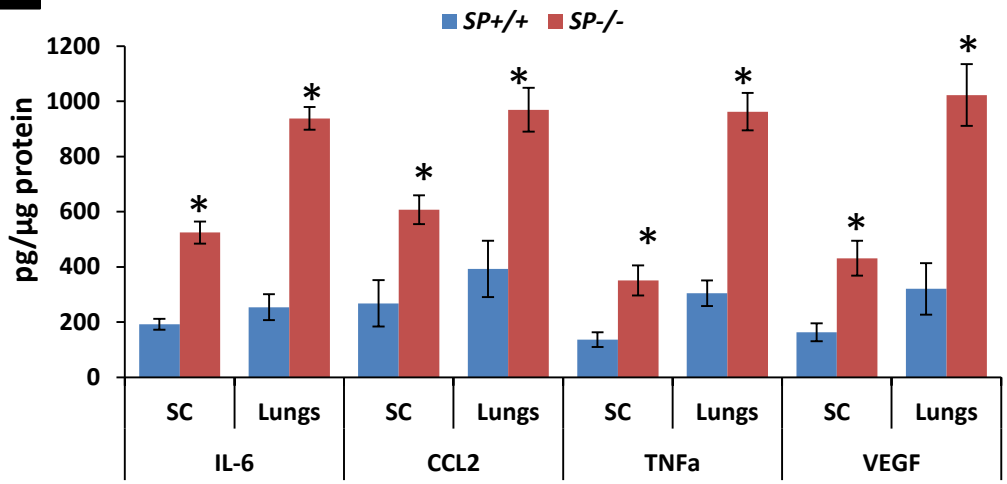

Supplement Figure 10

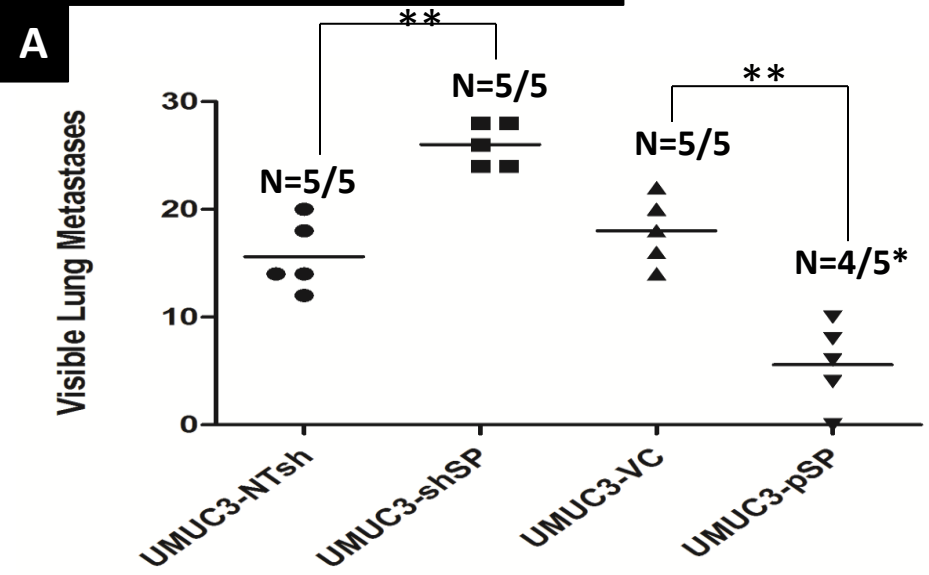

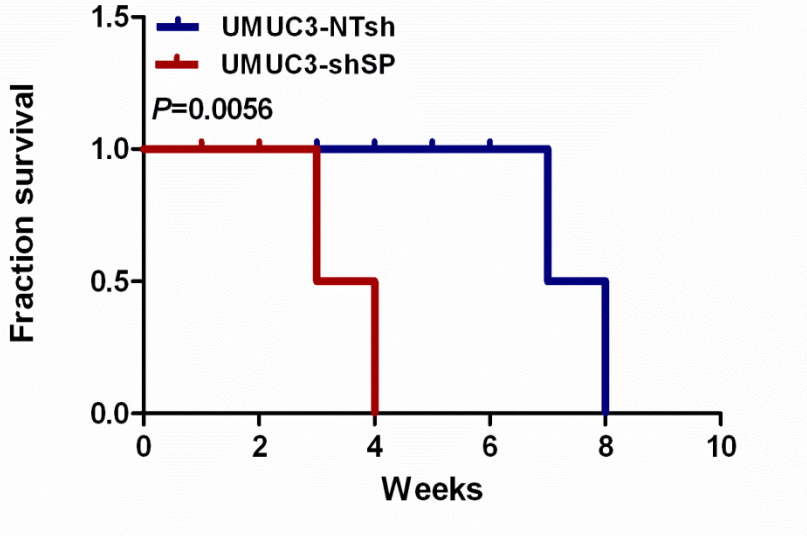

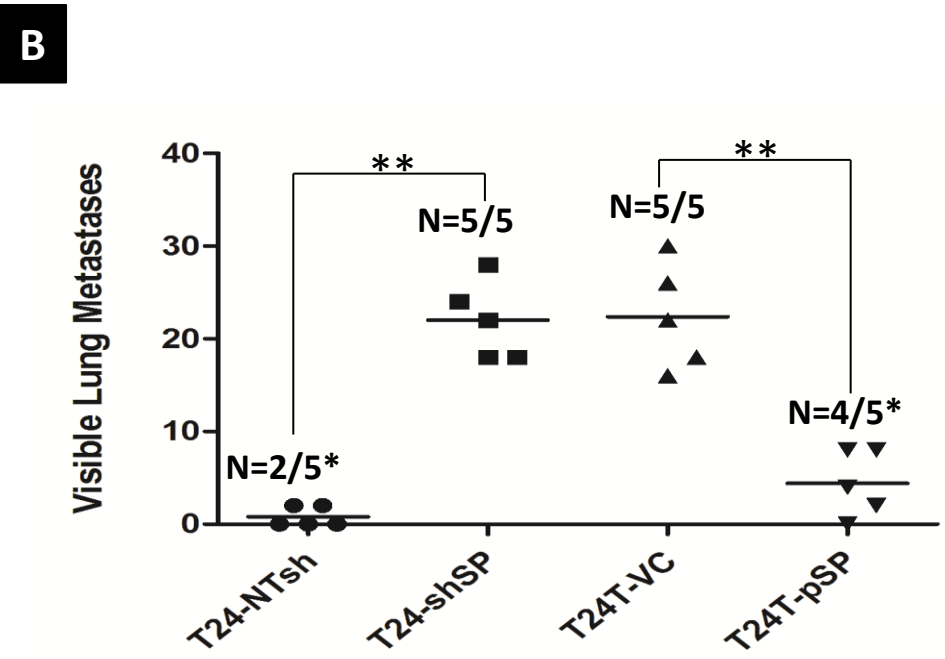

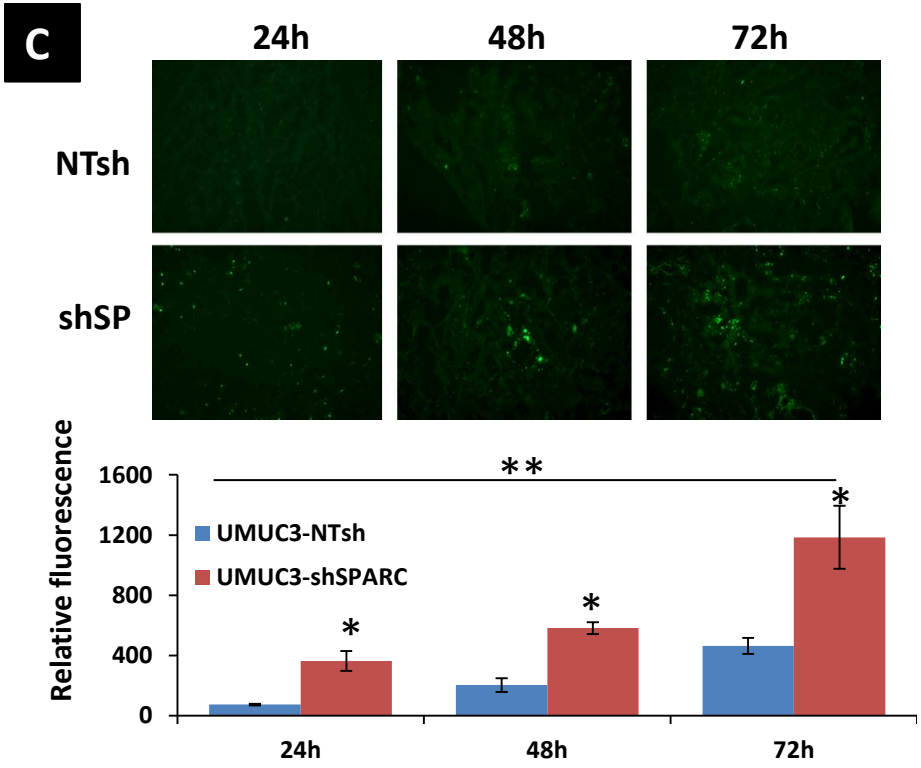

Supplement Figure 11

A

NMIUC

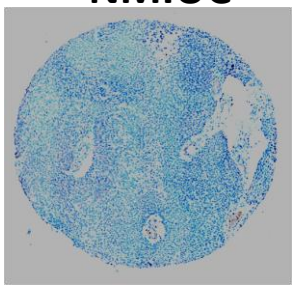

MIUC

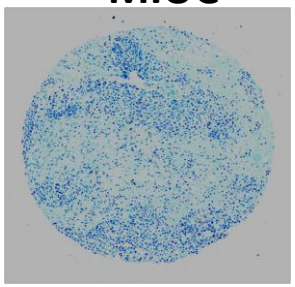

B

SPARC positive

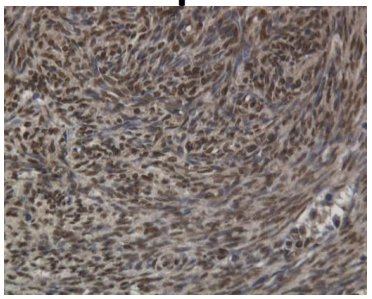

+ rhSP# 941-SP

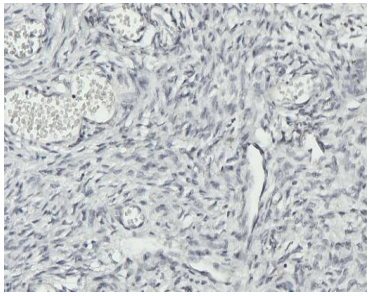

+ HON-0303

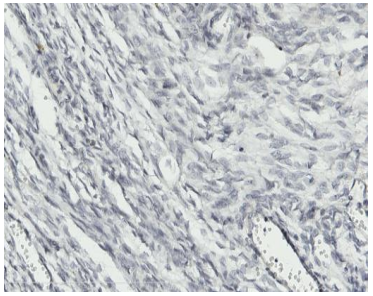

C

SPARC positive

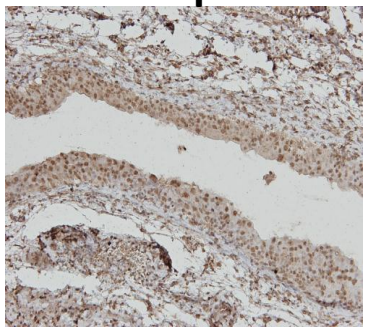

+ rmSPARC

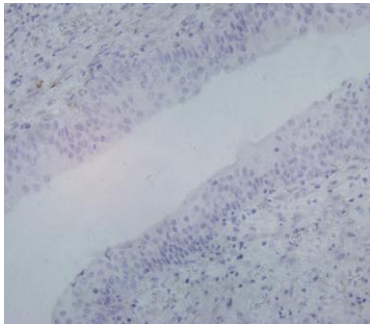

No 1°antibody

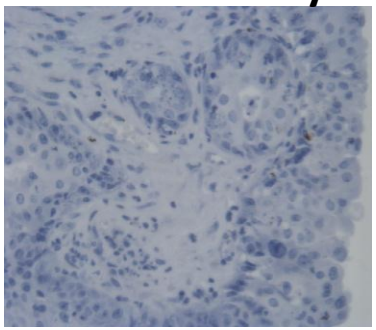

D

NU

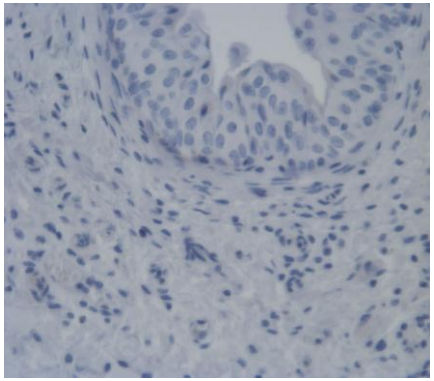

IAD

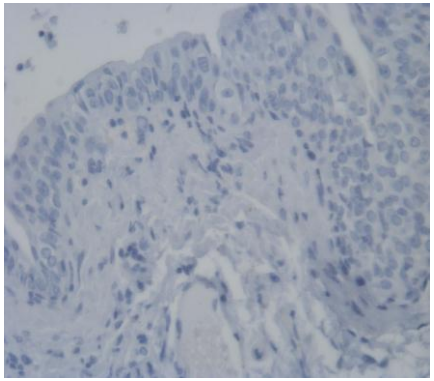

CIS

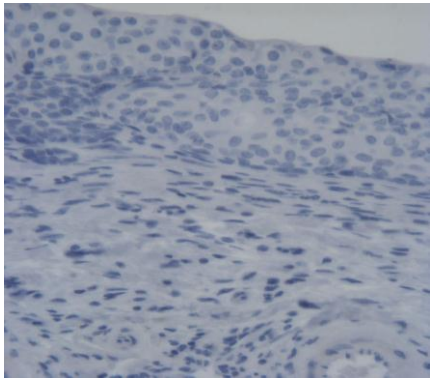

Invasive

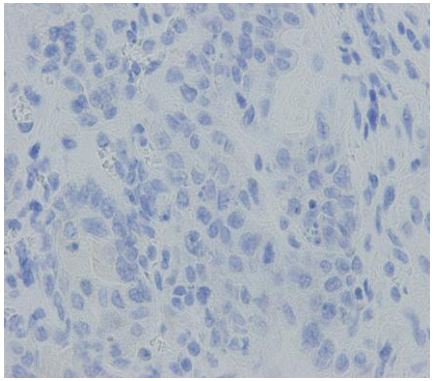

Supplement Figure 12